IEEE Photonics Journal
An IEEE Photonics Society Publication

Open Access

Enhancing Visibility of Polarimetric Underwater Image by Transmittance Correction

Volume 9, Number 3, June 2017

Haofeng Hu
Lin Zhao
Bingjing Huang
Xiaobo Li
Hui Wang
Tiegen Liu

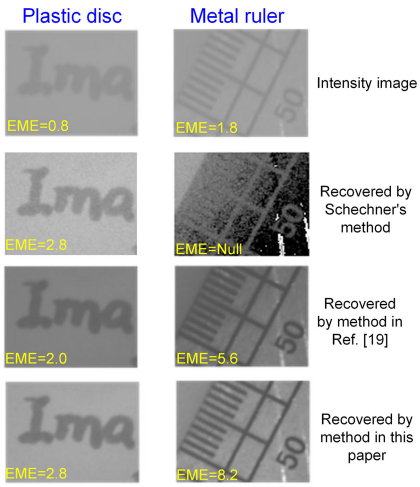

DOI: 10.1109/JPHOT.2017.2698000
1943-0655

IEEE photonics SOCIETY

IEEE

Enhancing Visibility of Polarimetric Underwater Image by Transmittance Correction

Haofeng Hu,[1,2] Lin Zhao,[1,2] Bingjing Huang,[1,2] Xiaobo Li,[1,2] Hui Wang,[1,2] and Tiegen Liu[1,2]

[1]College of Precision Instrument and Opto-Electronics Engineering, Tianjin University, Tianjin 300072, China
[2]Key Laboratory of Opto-Electronics Information Technology, Ministry of Education, Tianjin 300072, China

DOI:10.1109/JPHOT.2017.2698000

Manuscript received March 10, 2017; revised April 19, 2017; accepted April 22, 2017. Date of current version May 8, 2017. This work was supported in part by the National Natural Science Foundation of China under Grant 61405140, in part by the National Instrumentation Program under Grant 2013YQ030915, and in part by the Natural Science Foundation of Tianjin under Grant 15JCQNJC02000. Corresponding author: Haofeng Hu (e-mail: haofeng_hu@tju.edu.cn).

Abstract: Underwater vision can be severely degraded by the scattering media due to backscatter veiling and signal attenuation. In this paper, we focus on the case that the polarization effect of the object could not be neglected, and we propose a method for recovering the underwater image based on the transmittance correction, which transforms the transmittance for the low depolarized objects from negative values to the positive values that optimize the image quality with a simple algorithm of polynomial fitting. We show with a real-world experiment that with the method proposed in this paper, the quality of the underwater image can be effectively enhanced either for the object with high depolarization degree or for that with low depolarization degree. In particular, without sacrificing the quality of image recovery for the objects with high depolarization degree, the method proposed in this paper can achieve a better performance than the previous methods.

Index Terms: Polarimetric imaging, image enhancement, imaging through turbid media.

1. Introduction

The imaging quality of underwater scenes could be poor due to the disturbance of the turbid medium. The target signal can be partially absorbed and scattered by the particles in the water, which causes energy lost. Moreover, the undesired light scattered into the optical path by the particles causes the incoming light blending with the veiling light. The effects caused by absorption and scattering lead to the image quality reduction [1]. However, there are active demands for underwater image recovery, such as the exploration of marine resources and inspection of ship hulls for damage [2], [3]. Therefore, the effective way for recovering the underwater image is significant for these demands.

Previous methods for eliminating such negative effects of underwater imaging can be classified into two kinds: one is based on the computer visions, such as self-tuning restoration filter [4]; the other is based on physical models, such as dark channel prior [5] and polarimetric imaging [6]–[10], which is also used for dehazing [11]–[13]. The polarimetric imaging technique is well de-

veloped, and it can extremely improve the visibility of image by considering the polarization states of transmitted or backscattered light [14]–[16]. Some previews works of polarimetric imaging in turbid medium assumed a negligible degree of polarization (DOP) of the objects [6], [7], [11]. However, this assumption could not be appropriate for all cases, because the object radiance could also contribute to the polarization of the signal light. In particular, in the case that the depolarization degree of the objects is low, the signal light could be significantly polarized [17], [18], and thus there could be significant errors in the recovered image [19], [20]. In order to realize the underwater image recovery for the objects with low depolarization degrees, a method based on estimating the polarized-difference image of the target signal has been proposed in [19]. However, the estimation process is complex due to the introduction of nonlinear algorithm, and the computation is time consuming because there are multiple parameters to be optimized. In addition, it could sacrifice the image quality in regions of objects with low values of DOP. Therefore, a simpler and more effective method is still required.

In this paper, we investigate the relationship between the depolarization degree of the objects and the estimation of the medium transmittance. We propose an improved method for underwater image recovery based on the correction of the transmittance, which takes into account the contributions of both the object radiance and the veiling light to the polarization. In addition, the real world experiment of polarimetric imaging in the turbid water is performed, in order to demonstrate the superiority of the method both in the areas corresponding to the object with high DOP and the one with negligible DOP.

2. Optical Models

2.1 Model of Underwater Polarimetric Imaging

The basic physical model of image formation through the homogeneous turbid medium with active illumination is based on the model in [1], [7]. The image of the irradiance acquired by camera at the position (x, y) can be expressed as

$$I(x, y) = D(x, y) + B(x, y) \tag{1}$$

where $D(x, y)$ refers to the target signal which is attenuated due to absorption and scattering. $B(x, y)$ is called the veiling light or backscatter. The expressions of $D(x, y)$ and $B(x, y)$ are

$$D(x, y) = L(x, y)\, t(x, y) \tag{2}$$

$$B(x, y) = A_\infty [1 - t(x, y)] \tag{3}$$

where $L(x, y)$ is the radiance of the object without being attenuated, and A_∞ corresponds to the value of the backscatter in a line of sight that extends to infinity in the water. $t(x, y)$ is termed as the medium transmittance, which can be expressed as

$$t(x, y) = e^{-\beta(x,y)\rho(x,y)}. \tag{4}$$

The parameter $\beta(x, y)$ in (4) is the attenuation coefficient. In our case, we assume that the attenuation coefficient $\beta(x, y)$ is spatially invariant, which can be expressed as $\beta(x, y) = \beta_0$. Therefore, the transmittance $t(x, y)$ only depends on the propagation distance $\rho(x, y)$, which refers to the underwater part of the optical path between the object and the detector.

Based on the equations above, the transmittance $t(x, y)$ and the object radiance $L(x, y)$ can be deduced as

$$t(x, y) = 1 - \frac{B(x, y)}{A_\infty} \tag{5}$$

$$L(x, y) = \frac{I(x, y) - A_\infty [1 - t(x, y)]}{t(x, y)}. \tag{6}$$

By performing the analyzer at two orthogonal polarization states, we obtained a co-linear image $I^{\parallel}(x, y)$ with the analyzer at the same polarization state as the input polarization illumination, and a

cross-linear image $I^{\perp}(x, y)$ is obtained with the analyzer at the orthogonal state as the illumination. The total intensity of the acquired irradiance is

$$\begin{aligned} I(x, y) &= I^{\parallel}(x, y) + I^{\perp}(x, y) \\ &= \left[D^{\parallel}(x, y) + B^{\parallel}(x, y)\right] + \left[D^{\perp}(x, y) + B^{\perp}(x, y)\right]. \end{aligned} \tag{7}$$

Then the degree of polarization (DOP) of the backscatter can be described as [7], [21]

$$P_{scat}(x, y) = \frac{B^{\parallel}(x, y) - B^{\perp}(x, y)}{B^{\parallel}(x, y) + B^{\perp}(x, y)} = \frac{\Delta B(x, y)}{B(x, y)}. \tag{8}$$

According to (4), $t(x, y) \to 0$ when $\rho(x, y) \to \infty$. In this case, we can get

$$B(x, y) = A_{\infty}[1 - t(x, y)] \to A_{\infty} \tag{9}$$

$$P_{scat}(x, y) \to \frac{A_{\infty}^{\parallel} - A_{\infty}^{\perp}}{A_{\infty}^{\parallel} + A_{\infty}^{\perp}} = P_{scat}. \tag{10}$$

We assume the value of $P_{scat}(x, y)$ to be spatially constant [6], [7], and the expressions of transmittance can be written as

$$t(x, y) = 1 - \frac{\Delta B(x, y)}{P_{scat} A_{\infty}} \tag{11}$$

Substituting the expression of transmittance in (11) into (6), we can then deduce the object radiance $L(x, y)$.

In order to get the recovered image $L(x, y)$ according to the algorithm in (6), we need to estimate the global parameters A_{∞} as well as the transmittance $t(x, y)$. As indicated in (2) and (3), the attenuation of the signal and the backscatter significantly depend on the transmittance $t(x, y)$, and thus t(x,y) is a key parameter for recovering the underwater imaging.

2.2 Influence of Polarized Object on the Recovered Transmittance

It can be seen in (11) that $\Delta B(x, y)$ could have great impact on the accuracy of the estimation of the transmittance $t(x, y)$. Combing (7) and (8), $\Delta B(x, y)$ can be expressed as

$$\Delta B(x, y) = \Delta I(x, y) - \Delta D(x, y). \tag{12}$$

Then the transmittance $t(x, y)$ in (11) can be expressed as

$$t(x, y) = 1 - \frac{\Delta I(x, y)}{P_{scat} A_{\infty}} + \frac{\Delta D(x, y)}{P_{scat} A_{\infty}} \tag{13}$$

where $\Delta I(x, y)$ and $\Delta D(x, y)$ stand for the PD image of total intensity and the PD image of the target signal respectively.

In previews works [6], [7], [21], the polarization of the object radiance is ignored. In other words, $\Delta D(x, y)$ for the objects is considered to be 0. Therefore, the expression of the transmittance can be written as

$$t(x, y) = 1 - \frac{\Delta I(x, y)}{P_{scat} A_{\infty}} = 1 - \frac{I^{\parallel}(x, y) - I^{\perp}(x, y)}{P_{scat} A_{\infty}} \tag{14}$$

and the transmittance $t(x, y)$ can be obtained by simple pointwise computation. However, the polarization of object radiance may dominate over the partially polarized backscatter in some cases, such as in the region of the image corresponding to the smooth metal surfaces [18]. It can be seen from (13) that, in the regions corresponding to the objects with $\Delta D(x, y)$ greater than 0, the transmittance $t(x, y)$ without considering the polarization effect of the object can be considerably underestimated, which can even lead to the negative values of the transmittance t and thus the negative values of the object radiance L [19], [20]. Consequently, there could be considerable distortion in the recovered image in such situations.

Therefore, in order to deduce $L(x, y)$ properly, the key issue in our case is to estimate $t(x, y)$. In this paper, we proposed an improved method in the following to properly deduce the transmittance $t(x, y)$ and thus $L(x, y)$, and this method can be applied to the object which has complicated geometric shape without any prior knowledge.

3. Improved Algorithm of Underwater Image Recovery

3.1 Estimation of A_∞ and $\hat{P}_{scat}$

In order to recover the transmittance and the object radiance with (6) and (13), we need to estimate the global parameters A_∞ and P_{scat}, which are intrinsic parameters of the condition of underwater imaging. With the assumption that A_∞ and P_{scat} are spatially constant, we can directly measure A_∞ and P_{scat} from the images according to (9) and (10). In the position where the light propagates through enough scattering medium, the transmittance at the corresponding pixels is practically 0. Therefore, the most direct way of estimating A_∞ and P_{scat} is based on the measurement of the light intensity in a designated region belonging to the background in the acquired image, which is expressed as

$$\hat{A}_\infty = I_{back} \tag{15}$$

$$\hat{P}_{scat} = \frac{\Delta I_{back}}{I_{back}} \tag{16}$$

where the subscript back refers to the area of the background.

In practice, $\hat{P}_{scat}$ is often calculated according to a designated region in the background [21]. However, $\hat{P}_{scat}$ could vary slightly if one chooses different regions in the background, and thus there could be an error for estimation of $P_{scat}(x, y)$, which could affect the result of image recovery. Therefore, we employ the parameter ε to modify $\hat{P}_{scat}$ as $\varepsilon\hat{P}_{scat}$, in order to find an appropriate value of $\varepsilon\hat{P}_{scat}$ for image recovery.

3.2 The Method of Transmittance Correction

The physical range of the transmittance is from 0 to 1. It can be seen from (13) that the great values of $\Delta D(x, y)$ could cause the negative values of the transmittance $t(x, y)$. In other words, a patch with negative value of transmittance $t(x, y)$ corresponding to a high polarized object. In most cases, the depth at different positions of an object surface could not change much, which means the pixels of a surface are with almost same propagate distance $\rho(x, y)$ or transmittance $t(x, y)$.Therefore, we perform the intensity transformation on transmittance by the following algorithm:

$$t_{co}(x, y) = \begin{cases} t_{unco}(x, y), & t_{unco}(x, y) > t_{\inf} \\ t_{\inf}, & t_{unco}(x, y) \leq t_{\inf} \end{cases} \tag{17}$$

where $t_{co}(x, y)$ is the corrected transmittance and $t_{unco}(x, y)$ is the uncorrected transmittance deduced by (14). $t_{\inf}$ is the inflexion point of the intensity transformation function given by (17), which is shown in Fig. 1.

We consider the area in transmittance with negative values as a surface that with same depth. Therefore, we restrict the transmittance to a bound $t_{\inf}$. In the areas corresponding to the object with a negligible DOP, we operate the recovery algorithm according to (13) with $\Delta D(x, y) = 0$. However, there is a point of inflexion in the red curve corresponding to (17), which would cause the abrupt boundaries in the image due to the abrupt change of $t_{\inf}$ at the point of inflexion. In order to overcome this problem, we employ a polynomial function to fit the curve, as the blue dashed line shown in Fig. 1, and in this case, the change of $t_{\inf}$ at the point of inflexion is smooth. We employ the polynomial function for curve fitting because the polynomial function can be well consistent with the piecewise function given by (16), and in addition, the algorithm of polynomial function is simple, which decreases the complexity of calculation.

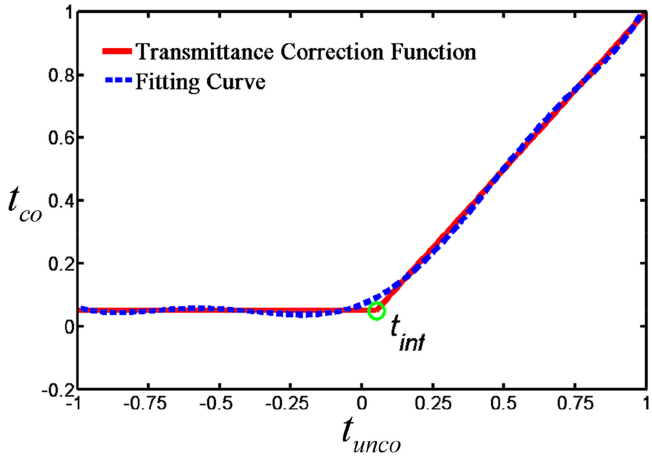

Fig. 1. Schematic of transmittance correction. The red curve presents (17), and the blue curve is the fitting curve.

In previous studies [6], [7], [12], the areas corresponding to the objects with negligible DOP can be recovered according to (6) and (14), and the effect of image recovery is ideal because the assumption that $\Delta D(x, y) = 0$ is correct. Therefore, a proper approach of image recovery is recovering the areas corresponding to the unpolarized objects with (6) and (14), while recovering the areas corresponds to the low depolarized objects with other methods. In fact, our method of transmittance correction illustrated above keeps the positive values in uncorrected transmittance almost unchanged, and we only correct the transmittance corresponding to the areas with low depolarized degree. In other words, our method recovers the areas corresponding to the unpolarized objects with (6) and (14). Therefore, it is expected that the recovery algorithm in this work could perform well in the areas that the depolarization degree of the object is high.

3.3 Optimization of Image Quality

With the estimation of A_∞ and P_{scat}, we can recover the underwater image according to (6). In order to correct the transmittance with (17), we need to figure out the value of the inflexion point t_{inf}. In addition, we also need to find an appropriate value of ε, which also has considerable impact on recovery algorithm.

In our study, the value of measure of enhancement (EME) is used to quantify the quality of the image [22], which is also used in [19] to evaluate the quality of the image, and EME is defined as

$$EME = \left| \frac{1}{k_1 k_2} \sum_{l=1}^{k_2} \sum_{k=1}^{k_1} 20 \log \frac{i^{\omega}_{\max;\,k,l}(x, y)}{i^{\omega}_{\min;\,k,l}(x, y) + q} \right|, \tag{18}$$

where the image is split up into $k_1 \times k_2$ blocks with the sequence number of (k, l) at two dimensions, while $i^{\omega}_{\max;\,k,l}(x, y)$ and $i^{\omega}_{\min;\,k,l}(x, y)$ are the maximum and minimum value in the blocks ω with sequence number of (k, l) in the image, and q (equals to 0.0001) is a small constant to avoid being divided by zero, without considerably modifying the result of EME. A high value of EME indicates a high quality of the image.

In order to optimize the quality of the recovered image, we perform an exhaustive search [10], [19], [23] of the coefficients t_{inf} and ε to find the optimal values of these coefficients that maximize the value of EME. Then we can get the corrected transmittance $t_{co}(x, y)$, and consequently, the object radiance $L(x, y)$ can be retrieved based on $t_{co}(x, y)$ by (6). It needs to be clarified that our goal is to recover the object radiance $L(x, y)$ given by (6), and we assume that $L(x, y)$ corresponds to the recovered image with optimal quality (with maximum value of EME).

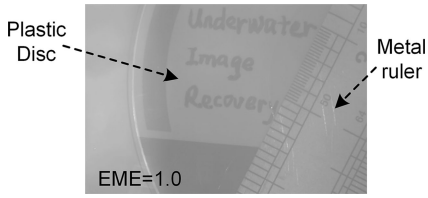

Fig. 2. Intensity image of the scene.

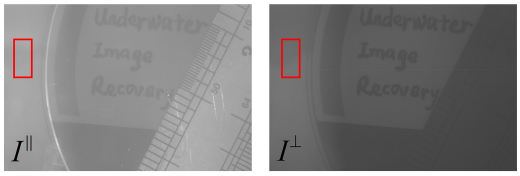

Fig. 3. (a) Co-linear image $I^{\parallel}(x, y)$. (b) Cross-linear image $I^{\perp}(x, y)$. The red square is the region belonging to the background, which is used to estimate the intensity of the backscatter at infinity and DOP of the backscatter.

4. Real-Word Experiment

We perform a real-world experiment of underwater imaging to verify the method of image recovery method illustrated in Section 3. The experimental setup is same to that in [19]. The light source is a He-Ne laser with the wavelength of 632.8 nm. The imaging device is a 14 bits digital CCD camera (AVT Stingray F-033B) with pixel number of 492 $\times$ 656. The illumination is modulated by a linear polarizer, and a rotating linear polarizer which is placed before CCD as an analyzer. We used a transparent PMMA tank filled with water, and we make the water turbid by blending the clear water with milk.

In our case, the target region consists of a metal ruler sticked on a plastic disc. The target is immersed in the turbid water, and the intensity image of this scene is shown in Fig. 2, with the value of EME calculated to be 1.0. It can be seen that the visibility of Fig. 2 is poor, and the details of the scene are severely degraded in the intensity image.

We obtain the images of $I^{\parallel}(x, y)$ and $I^{\perp}(x, y)$ at two orthogonal orientations of the polarizer before the CCD, as shown in Fig. 3.In order to estimate A_{∞} and P_{scat}, it is necessary to find a region in the image with no target to obtain $A_{\infty}^{\parallel}$ and $A_{\infty}^{\perp}$. In our experiments, this estimation is realized by averaging the intensity values in the designated region, which is indicated by the red rectangle in Fig. 3(a) and (b).

An important point that needs to be noticed in Fig. 3 is that there is a great difference between $I^{\parallel}(x, y)$ and $I^{\perp}(x, y)$ in the region corresponding to the metal ruler, while that for the disc is not so great. This indicates that the depolarization degree of the metal ruler is low, while that for the disc is high. The transmittance $t(x, y)$ calculated according to (14) with the assumption that $\Delta D(x, y) = 0$ is shown in Fig. 4. It can be seen in Fig. (4) that the calculated transmittance $t(x, y)$ is negative in the area of the ruler and at the edge of the disc, which is attributed to underestimating of ΔD in these areas.

As mentioned in Section 2.2, the method for deducing the transmittance based on (14) could be failed in the area corresponding to the metallic ruler which has high DOP, as shown in Fig. 4, in which the value of the transmittance t in the area of the metal ruler is negative. The theory of transmittance correction is illustrated in Section 3.2. In our experiment, the transmittance is corrected by a four order polynomial function which is achieved according to (17), and consequently, the deduction of object radiance $L(x, y)$ is performed according to (6). Since $t(x, y)$ is the function of t_{inf} and ε, $L(x, y)$ is also the function of t_{inf} and ε according to (6).

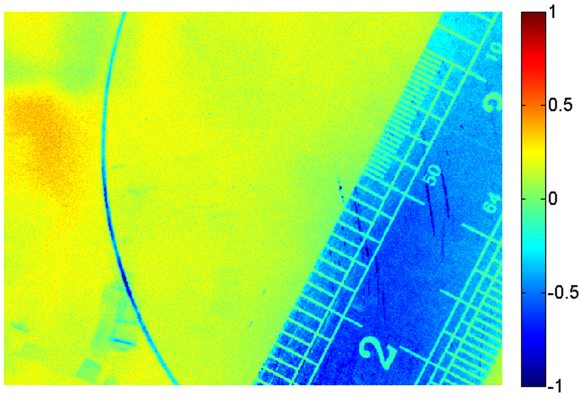

Fig. 4. Deduced transmittance $t(x, y)$ according to (14) with the assumption that $\Delta D(x, y) = 0$.

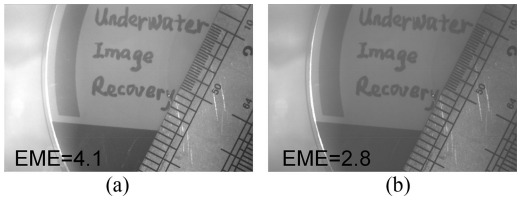

(a) (b)

Fig. 5. (a) Recovered image by the method of this paper with optimal values of t_{inf} and ε. (b) Recovered image by the method in [19].

For optimizing the quality of the recovered image, we perform the search of t_{inf} and ε to maximize the value of EME given by (18). The search was performed with a resolution step of 0.01 for both t_{inf} and ε. For our Matlab program running on the computer with Intel Core i5-3450 CPU@3.10 GHz processor, the iterative algorithm for the method proposed in this paper takes about 4 s for finding the optimal values of t_{inf} and ε. However for the same scenario, the Matlab program for the method proposed in [19] takes about 92 s for finding the optimal values of *a, b* and ε, which is much slower than that of the method proposed in this paper. This is because the method proposed in this paper is simpler and more effective due to decreasing one optimization coefficient, and thus it is more beneficial for real-time underwater image recovery. Consequently, we obtained the recovered image with optimal values of t_{inf} and ε($t_{\text{inf}} = 0.10$, $\varepsilon = 1.26$). Fig. 5(a) shows the retrieved radiance of the object $L(x, y)$ at optimal values of t_{inf} and ε. It can be seen that the visibility is greatly improved, and the image quality is enhanced to EME $= 4.1$. Compared with the intensity image [see Fig. 2], it can be seen in Fig. 5(a) that the images recovered by our method reveals the details of the scene that decay significantly in the intensity images, no matter for the area corresponding to the objects with high depolarization degree (plastic disc) or that with low depolarization degree (metal ruler). The image recovery result by the method in [19] is also presented in Fig. 5(b) for the purpose of comparison. It can be seen that the EME value of this method (EME $= 4.1$) is higher than that of [19] (EME $= 2.8$), which means that the quality of the recovered image for this method is better than that of [19].

In order to show the details of the image more clearly and to compare the effect of image recovery for different methods in more detail, we display in Fig. 6 the enlarged views of parts of the scene recovered by different methods. It can be seen in the left column of Fig. 6 that for the area of high depolarization degree (the area of the plastic disc), the performance of our method (with the EME of 2.8) is better than the performance of the method in [19] (with the EME of 2.0), and it is the same to that of Schechner's method [6]. This is because the method proposed in this paper process the area of high depolarization degree almost in the same way as that of Schechner's method [6], as illustrated in Fig. 1. In addition, it can be seen in the right column of Fig. 6 that for the area of low

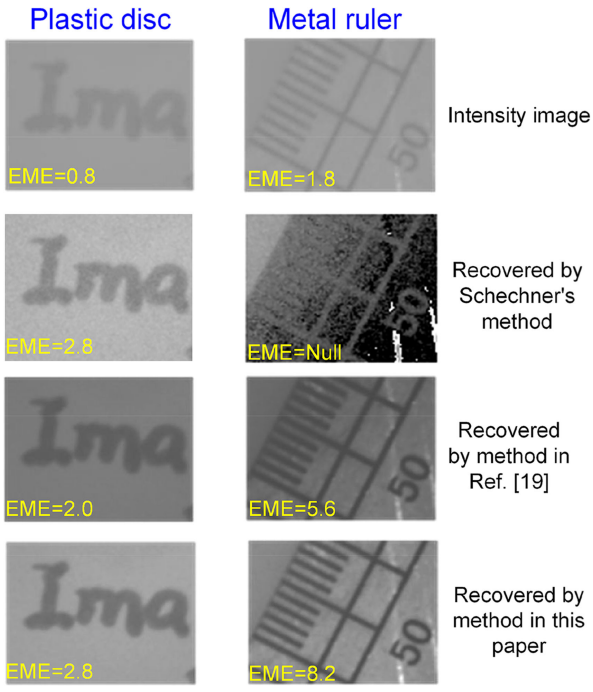

Fig. 6. Enlarged view of parts of the intensity image (see Fig. 2) and the recovered images by different methods, which correspond to the regions of plastic disc or metal ruler respectively.

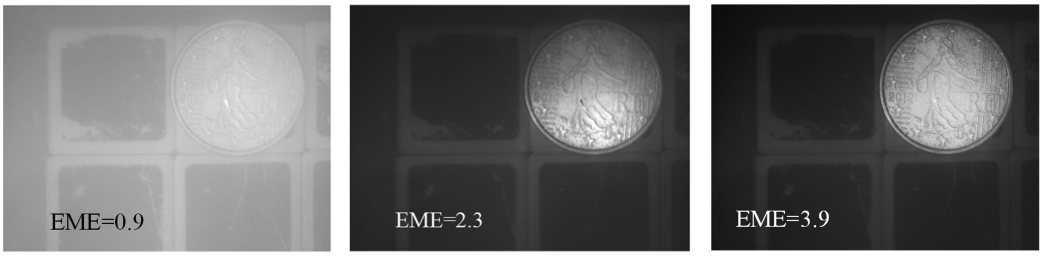

Fig. 7. (a) Intensity image of the scene. (b) Image recovered by method in [19]. (c) Image recovered by the method in this paper.

depolarization degree (the area of the metal ruler), the Schechner's method [6] is invalid, while the method in [19] can realize a relative good performance with EME of 5.6. However, the method in this paper has an even better performance with EME of 8.2.

The result in Fig. 6 indicates that the method proposed in this paper can realize the image recovery of the whole scene without sacrificing the recovery quality for the objects with high depolarization degree, and therefore, it can have a better performance than the method in [19], which is also shown in Fig. 5.

In order to verify the robustness of the method proposed by this paper, we perform another group of experiment, in which the target region consists of a plastic cube which refers to a low degree of polarization and a metal coin which refers to a high degree of polarization. The intensity image of the scene is shown in Fig. 7(a), and it can be seen that the details are severely degraded. By employing our method discussed in Section 3, the recovered image becomes more clear, and the image quality is enhanced to EME $=$ 3.9 shown in Fig. 7(c). The image recovered by the method in [19] (with the EME of 2.3) is also presented in Fig. 7(b) for the purpose of comparison.

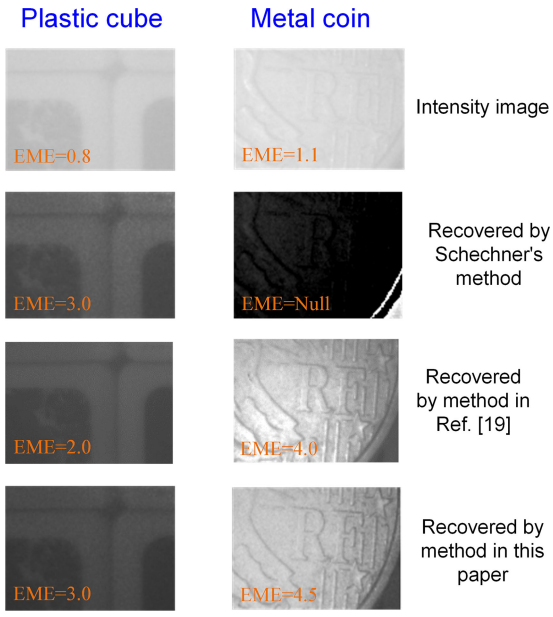

Fig. 8. Enlarged view of parts of the intensity image and the recovered images by different methods (see Fig. 7), which correspond to the regions of plastic cube or metal coin respectively.

In order to show the details of the image more clearly, we selected the objects with high depolarization degree (plastic cube) and low depolarization degree (metal coin) in the scene to compare with the method in [19]. The result in Fig. 8 demonstrates that the images recovered by the method of this paper also have a better performance (high value of EME) for high depolarization object and low depolarization object than Schechner's method [6] and the method in [19].

5. Conclusion

In this paper, we propose a method of underwater image recovery based on correction of the transmittance, which addresses successfully the issue of the vision in turbid media. The results of real-world experiment in this paper show that it is feasible to improve and optimize the quality of the recovered image by our method, and the detail information of the recovered image can be ameliorated. In particular, the experimental results show that our method could considerably improve the underwater images quality no matter the depolarization degree of the objects is high or low, while the Schechner's method [6], which is a classical method for image recovery in turbid media, could fail when the depolarization effect of the object is low. In addition, compared with the method proposed in [19], our method have two main advantages: 1) It can have a better image quality without sacrificing the quality of image recovery for the objects with high depolarization degree; 2) the algorithm is simpler than that in [19], and the computation is less time consuming.

Acknowledgment

H. Hu acknowledges the Fondation Franco-Chinoise pour la Science et ses Applications (FFCSA) and the China Scholarship Council (CSC).

References

[1] J. S. Jaffe, "Computer modeling and the design of optimal underwater imaging systems," *IEEE J. Ocean. Eng.*, vol. 15, no. 2, pp. 101–111, May 1990.

[2] G. N. Bailey and N. C. Flemming, "Archaeology of the continental shelf: Marine resources, submerged landscapes and underwater archaeology," *Quaternary Sci. Rev.*, vol. 27, pp. 2153–2165, 2008.
[3] L. B. Wolff, "Polarization vision: A new sensory approach to image understanding," *Image Vis. Comput.*, vol. 15, pp. 81–93, 1997.
[4] E. Trucco and A. T. Olmos-Antillon, "Self-tuning underwater image restoration," *IEEE J. Ocean. Eng.*, vol. 31, no. 2, pp. 511–519, Apr. 2006.
[5] K. He, J. Sun, and X. Tang, "Single image haze removal using dark channel prior," *IEEE Trans. Pattern Anal. Mach. Intell.*, vol. 33, no. 2, pp. 2341–2353, Dec. 2011.
[6] Y. Y. Schechner and N. Karpel, "Recovery of underwater visibility and structure by polarization analysis," *IEEE J. Ocean. Eng.*, vol. 30, no. 3, pp. 570–587, Jul. 2005.
[7] T. Treibitz and Y. Y. Schechner, "Active polarization descattering," *IEEE Trans. Pattern Anal. Mach. Intell.*, vol. 31, no. 3, pp. 385–399, Mar. 2009.
[8] M. Yu, T. Liu, H. Huang, H, Hu, and B. Huang, "Multispectral stokes imaging polarimetry based on color CCD," *IEEE Photon. J.*, vol. 8, no. 5, 2016, Art. no. 6900910.
[9] P. Wang, Q. Chen, G. Gu, W. Qian, and K. Ren, "Polarimetric image discrimination with depolarization mueller matrix," *IEEE Photon. J.*, vol. 8, no. 6, 2016, Art. no. 6901413.
[10] B. Huang, T. Liu, J. Han, and H. Hu, "Polarimetric target detection under uneven illumination," *Opt. Exp.*, vol. 23, no. 18, 2015, Art. no. 23603.
[11] Y. Y. Schechner, S. G. Narasimhan, and S. K. Nayar, "Polarization-based vision through haze," *Appl. Opt.*, vol. 42, pp. 511–525, 2003.
[12] J. Liang, L. Ren, H. Ju, W. Zhang, and E. Qu, "Polarimetric dehazing method for dense haze removal based on distribution analysis of angle of polarization," *Opt. Exp.*, vol. 23, pp. 26146–26157, 2015.
[13] J. Liang, L. Ren, H. Ju, E. Qu, and Y. Wang, "Visibility enhancement of hazy images based on a universal polarimetric imaging method," *J. Appl. Phys.*, vol. 116, 2014, Art. no. 173107.
[14] Q. Xu *et al.*, "A novel method of retrieving the polarization qubits after being transmitted in turbid media," *J. Opt.*, vol. 17, no. 3, 2015, Art. no. 035606.
[15] Q. Xu *et al.*, "Transmitting characteristics of polarization information under seawater," *Appl. Opt.*, vol. 54, no. 21, pp. 6584–6588, 2015.
[16] Q. Tao *et al.*, "Active imaging with the aids of polarization retrieve in turbid media system," *Opt. Commun.*, vol. 359, pp. 405–410, 2016.
[17] N. Agarwal *et al.*, "Spatial evolution of depolarization in homogeneous turbid media within the differential Mueller matrix formalism," *Opt. Lett.*, vol. 40, pp. 5634–5637, 2015.
[18] J. C. Stover, *Optical Scattering: Measurement and Analysis*. Bellingham, WA, USA: SPIE, 1995.
[19] B. Huang, T. Liu, H. Hu, J. Han, and M. Yu, "Underwater image recovery considering polarization effects of objects," *Opt. Exp.*, vol. 24, pp. 9826–9838, 2016.
[20] E. Namer and Y. Y. Schechner, "Advanced visibility improvement based on polarization filtered images," *Proc. SPIE*, vol. 5888, pp. 36–45, 2005.
[21] M. Dubreuil, P. Delrot, I. Leonard, A. Alfalou, C. Brosseau, and A. Dogariu, "Exploring underwater target detection by imaging polarimetry and correlation techniques," *Appl. Opt.*, vol. 52, pp. 997–1005, 2013.
[22] S. S. Agaian, K. Panetta, and A. M. Grigoryan, "Transform-based image enhancement algorithms with performance measure," *IEEE Trans. Image Process.*, vol. 10, no. 3, pp. 367–382, Mar. 2001.
[23] M. Boffety, H. Hu, and F. Goudail, "Contrast optimization in broadband passive polarimetric imaging," *Opt. Lett.*, vol. 39, pp. 6759–6762, 2014.